nance-enhanced Cu–OH–Cu modes in a number of other dinuclear copper complexes that lack phenolate or pyridine ligands[15,23,24] suggests that the presence of **both** types of ligands may be important. For the multicopper proteins of known structure, hemocyanin and ascorbate oxidase, histidine ligands abound and are likely to have similar vibronic properties to pyridine. However, there is no evidence for phenolate ligation of copper in these proteins. On the basis of our studies of the μ-OH-bridged copper complexes, we feel that it will be difficult to use Raman spectroscopy to detect bridging OH groups in these proteins.

Hydroxo-bridged dinuclear metal clusters are also of relevance to dinuclear iron proteins where they have been implicated in the mixed-valence forms of hemerythrin, purple acid phosphatase, and methane monooxygenase.[35] The μ-oxo bridge that is found in the fully oxidized forms of the dinuclear iron proteins is readily detected by RR spectroscopy.[25] The oxo → Fe(III) CT transition is a dominant chromophore in the near-UV region and leads to strong enhancement of the ν_s(Fe–O–Fe) mode. However, no such chromophoric character exists in the corresponding hydroxo-bridged complexes. We have been unable to detect ν_s(Fe–OH–Fe) in the RR spectra of hydroxo-bridged diiron(III) complexes containing pyrazole[36] or benzimidazole[37] ligands. We have observed an Fe–OH vibration in the RR spectrum of the dinuclear iron protein, purple acid phosphatase, that may arise from a bridging OH group.[38] Interestingly, this Fe–OH mode is resonance-enhanced via a phenolate → Fe(III) CT band. Therefore, it is likely that an additional strong chromophore such as that provided by a phenolate ligand is required in order to obtain RR spectra from hydroxo-bridged metal systems.

Acknowledgment. We are grateful to Dr. Nobumasa Kitajima for providing samples of the $Cu_2(L_2)(OH)_2$ complex[24a] and Dr. Roman Czernuszewicz for many helpful discussions. This work was supported by grants from the National Institutes of Health, Nos. GM 18865 (T.M.L. and J.S.-L.) and GM 28962 (K.D.K.).

---

(35) Sanders-Loehr, J. In *Iron Carriers and Iron Proteins*; Loehr, T. M., Ed.; VCH Publishers: New York, 1989; pp 375–466.

(36) Armstrong, W. H.; Lippard, S. J. *J. Am. Chem. Soc.* **1984**, *106*, 4632–4633.

(37) Ben-Hussein, A.; Gomez-Romero, P.; Morris, N. L.; Zafarullah, O.; Jameson, G. B. Personal communication.

(38) Backes, G.; Ling, J.; Loehr, T. M.; David, S.; Que, L., Jr.; Crowder, M. W.; Averill, B. A.; Sanders-Loehr, J. Unpublished results.

Contribution from the Department of Chemistry and Biochemistry,
University of South Carolina, Columbia, South Carolina 29208

Cluster Synthesis. 38. Formation of High-Nuclearity Platinum–Osmium Cluster Complexes. Synthesis, Structural Characterizations, and Interrelationships of $Pt_4Os_6(CO)_{22}(COD)$, $Pt_5Os_6(CO)_{21}(COD)_2$, $Pt_4Os_6(CO)_{19}(COD)_2$, and $Pt_7Os_6(CO)_{21}(COD)_2$ (COD = Cycloocta-1,5-diene)

Richard D. Adams,* Jau-Ching Lii, and Wengan Wu

Received December 27, 1991

Three new high-nuclearity platinum–osmium carbonyl cluster complexes $Pt_4Os_6(CO)_{22}(COD)$ (**2**), $Pt_5Os_6(CO)_{21}(COD)_2$ (**3**), and $Pt_4Os_6(CO)_{19}(COD)_2$ (**4**) were obtained in 17%, 13%, and 9% yields, respectively, from the pyrolysis of $Pt_2Os_3(CO)_{10}(COD)_2$ (**1**) under a CO atmosphere at 128 °C. Compounds **2**–**4** were characterized by IR, ^{1}H NMR, and single-crystal X-ray diffraction analyses. Compound **2** consists of two Pt_3Os_3 octahedra sharing a Pt_3 triangular face. A Pt(COD) group caps one of the Os_3 triangular faces. Compound **3** is structurally similar to compound **2** but has an additional Pt(COD) group capping one of the $PtOs_2$ triangular faces. The cluster of compound **4** can be viewed as a meta-bicapped Pt_2Os_4 octahedron with an additional Pt(COD) group capping a $PtOs_2$ triangle to one of the capping groups on the octahedron and a Pt(COD) group bridging the Pt–Pt edge of the octahedron. Compound **2** was converted to **4** in 65% yield, when it was irradiated in the presence of COD. When compound **2** was treated with 1 equiv of trimethylamine *N*-oxide and 2 equiv of $Pt(COD)_2$, compound **3** and a new higher nuclearity platinum–osmium carbonyl complex $Pt_7Os_6(CO)_{21}(COD)_2$ (**5**; 8% yield) were obtained. Compound **5** was characterized by a single-crystal X-ray diffraction analysis. It was formed by the loss of one CO from **2** and the addition of three Pt atoms and one COD ligand. The structure consists of layers of metal atoms. A platinum-capped Os_3 triangle sits next to a planar Pt_4 layer, which in turn lies next to a planar five atom layer consisting of three osmium and two platinum atoms. Compound **2** was converted to the known compound $Pt_4Os_6(CO)_{21}(COD)(\mu\text{-}H)_2$ (**6**) in good yield (79%) by reacting with trimethylamine *N*-oxide and hydrogen. Crystal data: for **2**, space group $P2_1/n$, $a = 20.404$ (6) Å, $b = 9.607$ (5) Å, $c = 24.171$ (8) Å, $\beta = 90.512$ (3)°, $Z = 4$, and $R = 0.040$ for 2847 reflections; for **3**, space group $P2_1/m$, $a = 12.023$ (8) Å, $b = 16.010$ (9) Å, $c = 13.902$ (7) Å, $\beta = 103.79$ (5)°, $Z = 2$, and $R = 0.037$ for 2428 reflections; for **4**, space group $C2/c$, $a = 45.67$ (1) Å, $b = 11.836$ (4) Å, $c = 17.444$ (4) Å, $\beta = 99.04$ (2)°, and $R = 0.034$ for 3295 reflections; for **5**, space group $P2_1/n$, $a = 21.061$ (6) Å, $b = 12.086$ (3) Å, $c = 21.348$ (6) Å, $\beta = 92.06$ (2)°, and $R = 0.039$ for 3134 reflections.

Introduction

The chemistry of heteronuclear cluster complexes containing platinum has attracted a great deal of interest[1] because of the importance of platinum alloys to the process of catalytic petroleum re-forming.[2] Higher nuclearity mixed-metal clusters may serve as good models for such catalysts because the arrangement of the metal atoms on their surfaces may resemble those on the surfaces of real catalysts. To date, however, there are relatively few examples of high-nuclearity mixed-metal cluster complexes con-

---

(1) (a) Farrugia, L. J. *Adv. Organomet. Chem.* **1990**, *31*, 301. (b) Braunstein, P.; Rose, J. In *Stereochemistry of Organometallic and Inorganic Compounds*; Bernal, I., Ed.; Elsevier: Amsterdam, 1989; Vol. 3.

(2) (a) Sinfelt, J. H. *Bimetallic Catalysts. Discoveries, Concepts and Applications*; Wiley: New York, 1983. (b) Sinfelt, J. H. *Sci. Am.* **1985**, *253*, 90. (c) Sinfelt, J. H. *Acc. Chem. Res.* **1977**, *10*, 15. (d) Sachtler, W. M. H. *J. Mol. Catal.* **1984**, *25*, 1. (e) Ponec, V. *Adv. Catal.* **1983**, *32*, 149. (f) Biswas, J.; Bickle, G. M.; Gray, P. G.; Do, D. D.; Barbier, J. *Catal. Rev.—Sci. Eng.* **1988**, *30*, 161.

Table I. Crystallographic Data for Diffraction Studies

	compd			
	2	**3**	**4**	**5**
empirical formula	$Pt_4Os_6O_{22}C_{30}H_{12}\cdot1.5C_6H_6$	$Pt_5Os_6O_{21}C_{37}H_{24}\cdot C_6H_6$	$Pt_4Os_6O_{19}C_{35}H_{24}\cdot0.5C_6H_6$	$Pt_7Os_6O_{21}C_{37}H_{24}\cdot CH_2Cl_2$
fw	2763.14	2999.35	2709.18	3396.35
cryst system	monoclinic	monoclinic	monoclinic	monoclinic
lattice params				
a, Å	20.404 (6)	12.023 (8)	45.67 (1)	21.061 (6)
b, Å	9.607 (5)	16.010 (9)	11.836 (4)	12.086 (3)
c, Å	24.171 (8)	13.902 (7)	17.444 (4)	21.348 (6)
β, deg	90.512 (3)	103.79 (5)	99.04 (2)	92.06 (2)
V, Å^3	4738 (5)	2599 (5)	9313 (4)	5430 (2)
space group	$P2_1/n$ (No. 14)	$P2_1/m$ (No. 11)	$C2/c$ (No. 15)	$P2_1/n$ (No. 14)
Z	4	2	8	4
D_{calc}, g/cm^3	3.87	3.84	3.86	4.15
μ(Mo, Kα), cm^{-1}	280.0	282.4	284.8	323.0
abs corr	empirical	empirical	analytical	analytical
temp, °C	20	20	20	20
no. of observns ($I > 3\sigma(I)$)	2847	2428	3295	3134
no. of variables	335	256	409	362
residuals:[a] R, R_w	0.040, 0.040	0.037. 0.040	0.034, 0.033	0.039, 0.037

[a] $R = \sum_{hkl}(||F_o| - |F_c||)/\sum|F_o|$; $R_w = (\sum_{hkl}w(|F_o| - |F_c|)^2/\sum_{hkl}w|F_o|^2)^{1/2}$.

taining platinum.[3-6] We have recently discovered new synthetic routes to high-nuclearity platinum–osmium and platinum–ruthenium carbonyl cluster complexes.[7] We have now found that the pyrolysis of $Pt_2Os_3(CO)_{10}(COD)_2$ (**1**) at 128 °C yields three new high-nuclearity platinum–osmium carbonyl cluster complexes $Pt_4Os_6(CO)_{22}(COD)$ (**2**), $Pt_5Os_6(CO)_{21}(COD)_2$ (**3**), and $Pt_4Os_6(CO)_{19}(COD)_2$ (**4**). Compound **2** can be enlarged by further reaction with $Pt(COD)_2$ to produce **3** and the 13-metal cluster complex $Pt_7Os_6(CO)_{21}(COD)_2$ (**5**). When decarbonylated by Me_3NO, compound **2** reacts with hydrogen to give the known compound $Pt_4Os_6(CO)_{21}(COD)(H)_2$[6c] (**6**) in high yield. The results of this study are described in this report. A preliminary report of this work has been published.[6b]

Experimental Section

General Procedures. All the reactions were performed under an atmosphere of nitrogen, unless otherwise indicated. Reagent grade solvents were dried over molecular sieves and were deoxygenated by purging with nitrogen prior to use. $Pt(COD)_2$[8a] and $Pt_2Os_3(CO)_{10}(COD)_2$[8b] were prepared by the reported procedures. $Me_3NO\cdot2H_2O$ was purchased from Aldrich and was dehydrated by the published procedure before use.[9] UV irradiation was performed by using an 85-W external high-pressure mercury lamp. TLC separations were performed in air on plates (0.25 mm, silica gel 60 F_{254}). IR spectra were recorded on a Nicolet 5 DXB FT-IR spectrophotometer. ^1H NMR spectra were recorded on a Bruker AM-300 spectrometer. Elemental analyses were performed at Desert Analytics, Tucson, AZ, for C and H and at Oneida Research Services, Whitesboro, NY, for Pt.

Pyrolysis of $Pt_2Os_3(CO)_{10}(COD)_2$ (1). A 39.0-mg amount of **1** was packed in two glass capillaries and sealed under carbon monoxide (1 atm). The capillaries were heated at 128 °C for 2 min. The products were isolated by dissolving the solid in a minimum amount CH_2Cl_2 and transferring the solution to TLC plates and eluting it with a hexane/CH_2Cl_2 (3/2) solvent mixture. The products eluted in the following order: $PtOs_2(CO)_8(COD)$[6a] (yellow, trace), $Pt_2Os_4(CO)_{18}$[10] (red, 1.4 mg, 4%), $Pt_2Os_4(CO)_{17}$[6d] (green, 1.2 mg, 4%), $Pt_2Os_4(CO)_{12}(COD)_2$[6a] (red-brown, 2.6 mg, 8%), $Pt_4Os_6(CO)_{22}(COD)$ (**2**, brown, 5.9 mg, 17%), unknown (**7**, orange, 0.6 mg), $Pt_2Os_6(CO)_{17}(COD)_2$[5a] (brown, trace), $Pt_5Os_6(CO)_{21}(COD)_2$ (**3**, dark-brown, 4.0 mg, 13%), and $Pt_4Os_6(CO)_{19}(COD)_2$ (**4**, light-brown, 3.2 mg, 9%). IR (ν(CO), cm^{-1}, in CH_2Cl_2): for **2**, 2092 (w), 2053 (vs), 2041 (vs), 2021 (w, sh), 1967 (w, br), 1845 (w, vbr); for **3**, 2074 (m), 2041 (s, sh), 2033 (vs), 2023 (s), 1986 (w, br), 1959 (w, br); for **4**, 2080 (m), 2044 (vs), 2026 (m), 2016 (w, sh), 1991 (w, sh), 1984 (w, br); for **7**, 2097 (w), 2066 (s), 2045 (vs), 2033 (w, sh), 1980 (vw, br). ^1H NMR (δ in $CDCl_3$, unless otherwise indicated): for **2**, 6.00 (t, CH, J_{Pt-H} = 58 Hz), 2.20–2.70 (br, CH_2); for **3**, 2.10–2.75 (br, CH_2); for **4** in C_6D_6, 0.8–1.4 (br, CH_2). Anal. Calcd (found) for **2**: Pt, 29.49 (29.19); C, 13.62 (13.38); H, 0.46 (0.48). Calcd (found) for **3**-C_6H_6: Pt, 32.54 (30.74); C, 17.22 (15.99); H, 1.01 (0.78). Calcd (found) for **4**: C, 15.74 (15.81); H, 0.91 (0.86).

Reaction of 2 with $Pt(COD)_2$ and Trimethylamine *N*-Oxide. In a typical reaction 11.0 mg of **2** was dissolved in 10 mL of CH_2Cl_2 in a 25-mL three-necked flask. The solution was cooled at 0 °C, and 1 equiv of Me_3NO was added. The IR spectrum changed immediately, and 2 equiv of $Pt(COD)_2$ was then added at 0 °C. The solution was stirred for 30 min and then concentrated and separated by TLC using a hexane/CH_2Cl_2 (3/2) solvent mixture. The products eluted in the following order: **2** (1.2 mg), brown $Pt_7Os_6(CO)_{21}(COD)_2$ (**5**; 1.0 mg, 8%), and **3** (0.6 mg, 6%). Data for **5** are as follows. IR (ν(CO), cm^{-1}, in CH_2Cl_2): 2076 (m), 2052 (m), 2040 (vs), 2031 (s), 2001 (w), 1979 (w, br). ^1H NMR (δ in C_6D_6): 0.8–1.4 (br, CH_2). Anal. Calcd (found): Pt, 41.24 (41.50).

Photolysis of 2 with Cyclooctadiene. A 7.7-mg amount of **2** and 2 equiv of cycloocta-1,5-diene were dissolved in 20 mL of CH_2Cl_2 in a 50-mL three-necked Pyrex flask. The solution was photolyzed by using an externally positioned 85-W high-pressure UV lamp with a slow purge of nitrogen for a period of 2 days.

---

(3) (a) Fumagalli, A.; Martinengo, S.; Ciani, G. *J. Organomet. Chem.* **1984**, *273*, C46. (b) Fumagalli, A.; Martinengo, S.; Ciani, G. *J. Chem. Soc., Chem. Commun.* **1983**, 1381. (c) Fumagalli, A.; Martinengo, S.; Ciani, G.; Marturano, G. *Inorg. Chem.* **1986**, *25*, 592.

(4) (a) Ceriotti, A.; Demartin, F.; Longoni, G.; Manassero, M.; Marchionna, M.; Piva, G.; Sansoni, M. *Angew. Chem., Int. Ed. Engl.* **1985**, *24*, 697. (b) Longoni, G.; Manassero, M.; Sansoni, M. *J. Am. Chem. Soc.* **1980**, *102*, 7973. (c) Ceriotti, A.; Demartin, F.; Longoni, G.; Manassero, M.; Piva, G.; Piro, G.; Sansoni, M.; Heaton, B. T. *J. Organomet. Chem.* **1986**, *301*, C5.

(5) (a) Couture, C.; Farrar, D. H.; Goudsmit, R. J. *Inorg. Chim. Acta* **1984**, *89*, L29. (b) Couture, C.; Farrar, D. H. *J. Chem. Soc., Chem. Commun.* **1985**, 197. (c) Couture, C.; Farrar, D. H. *J. Chem. Soc., Dalton Trans.* **1987**, 2245. (d) Couture, C.; Farrar, D. H. *J. Chem. Soc., Dalton Trans.* **1987**, 2253.

(6) (a) Adams, R. D.; Wu, W. *Inorg. Chem.* **1991**, *30*, 3605. (b) Adams, R. D.; Lii, J. C.; Wu, W. *Inorg. Chem.* **1991**, *30*, 2257. (c) Adams, R. D.; Lii, J. C.; Wu, W. *Inorg. Chem.* **1991**, *30*, 3613. (d) Adams, R. D.; Alexander, M. S.; Arafa, I.; Wu, W. *Inorg. Chem.* **1991**, *30*, 4717.

(7) (a) Adams, R. D.; Arafa, I.; Chen, G.; Lii, J. C.; Wang, J. G. *Organometallics* **1990**, *9*, 2350. (b) Adams, R. D.; Chen, G.; Wang, J. G.; Wu, W. *Organometallics* **1990**, *9*, 1339. (c) Adams, R. D.; Pompeo, M. P.; Wu, W. *Inorg. Chem.* **1991**, *30*, 2899.

(8) (a) Spencer, J. L. *Inorg. Synth.* **1979**, *19*, 213. (b) Adams, R. D.; Chen, G.; Lii, J. C.; Wu, W. *Inorg. Chem.* **1991**, *30*, 1007.

(9) Smith, C.; Boekelheide. In *Organic Synthesis*; Wiley: New York, 1973; Collect. Vol. V, p 872.

(10) (a) Sundberg, P. *J. Chem. Soc., Chem. Commun.* **1987**, 1307. (b) Adams, R. D.; Pompeo, M. P.; Wu, W. *Inorg. Chem.* **1991**, *30*, 2425.

During the first 10 h, five additions of COD (2 equiv/addition) were made to the reaction solution at 2-h intervals. At the end the solvent was removed under vacuum. The residue was dissolved in a minimum amount of CH_2Cl_2 and separated by TLC using a solvent mixture of hexane/CH_2Cl_2 (3/2). A 1.6-mg amount of **2** was recovered, and 4.0 mg of **4** (65% yield) was obtained.

Reaction of 2 and H_2 in the Presence of Trimethylamine *N*-Oxide. A 6.5-mg amount of **2** was dissolved in 15 mL of CH_2Cl_2 in a 25-mL three-necked flask. A 1-equiv sample of Me_3NO was added, and the solution was purged slowly with H_2. The solution was stirred at 25 °C for 18 h. The solvent was removed under vacuum. The product was isolated by TLC by using a solvent mixture of hexane/CH_2Cl_2 (1/1) to yield 5.1 mg of $Pt_4Os_6(CO)_{21}(COD)(\mu\text{-}H)_2$ (**6**; 79%).

Crystallographic Analyses. Opaque dark crystals **2**–**5** were grown by slow evaporation of solvent from solution in a 7/3 CH_2Cl_2/benzene solvent mixture at 25 °C. All data crystals were mounted in thin-walled glass capillaries. Diffraction measurements were made on a Rigaku AFC6S fully-automated four-circle diffractometer using molybdenum Kα radiation. Unit cells were determined and refined from 15 randomly selected reflections obtained by using the AFC6S automatic search, center, index, and least-squares routines. Crystal data, data collection parameters, and results of the analyses are listed in Table I. The data were processed on a Digital Equipment Corp. VAXstation 3520 computer by using the TEXSAN structure solving library, Version 5.0, obtained from the Molecular Structure Corp., The Woodlands, TX. The data were corrected for Lorentz and polarization effects (Lp) and absorption. Neutral-atom scattering factors were calculated by the standard procedures.[11a] Anomalous dispersion corrections were applied to all non-hydrogen atoms.[11b] All of the structures were solved by a combination of direct methods (MITHRIL) and difference Fourier syntheses. Full-matrix least-squares refinements minimized the function $\sum_{hkl} w(|F_o| - |F_c|)^2$, where $w = 1/\sigma(F)^2$, $\sigma(F) = \sigma(F^2_o)/2F_o$, and $\sigma(F^2_o) = [\sigma(I_{raw})^2 + (0.02I_{net})^2]^{1/2}/Lp$.

For each of the structures the hydrogen atoms on the COD ligands were calculated in idealized positions and were added in the structure factor calculations without refinement.

Compound **2** crystallized in a monoclinic crystal system. The space group $P2_1/n$ was identified on the basis of the systematic absences observed during the collection of the data. All metal atoms were refined with anisotropic thermal parameters. The carbon and oxygen atoms were refined isotropically. The crystal was found to contain one and one-half molecules benzene in the asymmetric crystal unit that had cocrystallized from the crystallization solvent. One of these lay on a crystallographic center of symmetry. Both molecules were included in the analysis and satisfactorily refined.

Compound **3** crystallized in a monoclinic crystal system. The systematic absences observed during the collection of data were consistent with either of the space groups $P2_1/m$ or $P2_1$. The centrosymmetric space group was assumed and confirmed by the successful solution and refinement of the structure. The lattice was found to contain only two formula equivalents of the complex in the unit cell and the molecule is thus required to contain crystallographic reflection symmetry. All atoms heavier than carbon were refined anisotropically. The carbon atoms were refined with isotropic thermal parameters. The crystal was found to contain half of a molecule of benzene in the asymmetric crystal unit that had cocrystallized from the crystallization solvent. It was positioned on a crystallographic center of symmetry. It was included in the analysis and satisfactorily refined.

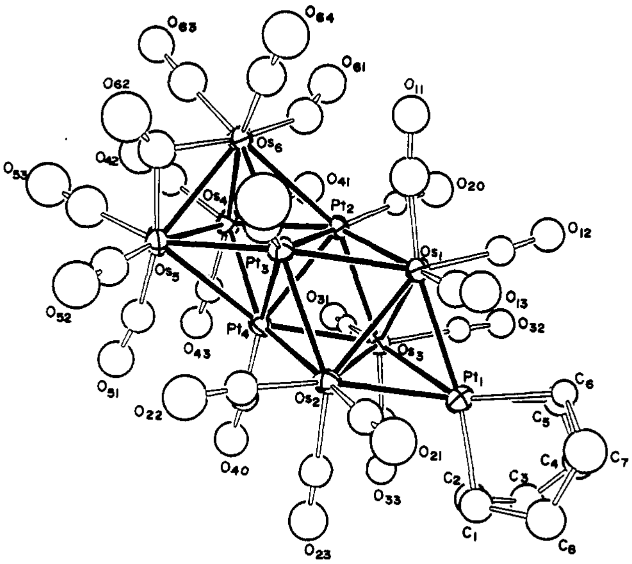

Figure 1. ORTEP drawing of $Pt_4Os_6(CO)_{22}(COD)$ (**2**), showing 50% probability thermal ellipsoids.

Table II. Positional Parameters and *B*(eq) Values for $Pt_4Os_6(CO)_{22}(C_8H_{12})$ (**2**)

atom	*x*	*y*	*z*	*B*(eq), Å^2
Pt(1)	0.663 31 (07)	0.762 82 (16)	0.423 68 (06)	2.89 (7)
Pt(2)	0.524 77 (07)	0.901 60 (14)	0.276 05 (06)	2.30 (7)
Pt(3)	0.462 07 (07)	0.703 34 (15)	0.329 30 (06)	2.58 (7)
Pt(4)	0.554 09 (07)	0.631 91 (15)	0.259 50 (06)	2.62 (7)
Os(1)	0.546 97 (07)	0.877 59 (15)	0.388 48 (06)	2.49 (7)
Os(2)	0.577 77 (07)	0.587 35 (15)	0.370 44 (06)	2.74 (7)
Os(3)	0.645 90 (07)	0.805 09 (15)	0.302 79 (06)	2.40 (7)
Os(4)	0.489 36 (07)	0.779 82 (17)	0.173 62 (06)	2.99 (8)
Os(5)	0.417 06 (07)	0.567 60 (16)	0.232 50 (07)	3.28 (8)
Os(6)	0.386 22 (07)	0.846 87 (16)	0.248 38 (06)	2.86 (8)

Table III. Intramolecular Distances for **2**[a]

Pt(1)–Os(1)	2.745 (2)	Pt(3)–Os(6)	2.841 (2)
Pt(1)–Os(2)	2.739 (2)	Pt(4)–Os(2)	2.754 (3)
Pt(1)–Os(3)	2.969 (2)	Pt(4)–Os(3)	2.709 (2)
Pt(2)–Pt(3)	2.636 (2)	Pt(4)–Os(4)	2.833 (2)
Pt(2)–Pt(4)	2.690 (2)	Pt(4)–Os(5)	2.931 (2)
Pt(2)–Os(1)	2.761 (2)	Os(1)–Os(2)	2.892 (3)
Pt(2)–Os(3)	2.712 (2)	Os(1)–Os(3)	2.987 (2)
Pt(2)–Os(4)	2.826 (2)	Os(2)–Os(3)	3.004 (2)
Pt(2)–Os(6)	2.946 (2)	Os(4)–Os(5)	2.897 (2)
Pt(3)–Pt(4)	2.627 (2)	Os(4)–Os(6)	2.859 (2)
Pt(3)–Os(1)	2.794 (2)	Os(5)–Os(6)	2.783 (3)
Pt(3)–Os(2)	2.786 (2)	O–C(av)	1.18 (5)
Pt(3)–Os(5)	2.825 (2)		

[a] Distances are in angstroms. Estimated standard deviations in the least significant figure are given in parentheses.

Compound **4** crystallized in a monoclinic crystal system. The systematic absences observed during the collection of data were consistent with either of the space groups $C2/c$ or Cc. The centrosymmetric space group $C2/c$ was assumed and confirmed by the successful solution and refinement of the structure. All atoms larger than carbon were refined anisotropically. The carbon atoms were refined with isotropic thermal parameters. The crystal was found to contain half of a molecule of benzene in the asymmetric crystal unit that had cocrystallized from the crystallization solvent. It was positioned on a crystallographic center of symmetry. It was included in the analysis and satisfactorily refined.

Compound **5** crystallized in a monoclinic crystal system. The space group $P2_1/n$ was identified on the basis of the systematic absences observed during the collection of the data. All metal atoms were refined with anisotropic thermal parameters. The carbon and oxygen atoms were refined isotropically. In the final stages of refinement a molecule of CH_2Cl_2 that had cocrystallized from the crystallization solvent was located in the lattice. It was included in the analysis and satisfactorily refined.

Results and Discussion

From pyrolysis of solid $Pt_2Os_3(CO)_{10}(COD)_2$ (**1**) under an atmosphere of CO at 128 °C, we have obtained three new mixed-metal cluster complexes $Pt_4Os_6(CO)_{22}(COD)$ (**2**), Pt_5Os_6(C-

---

(11) *International Tables for X-ray Crystallography*; Kynoch Press: Birmingham, England, 1975; Vol. IV: (a) Table 2.2B, pp 99–101; (b) Table 2.3.1, pp 149–150.

Table IV. Intramolecular Bond Angles[a]

Pt(3)–Pt(2)–Pt(4)	59.09 (6)	Pt(2)–Pt(4)–Pt(3)	59.45 (6)
Pt(3)–Pt(2)–Os(1)	62.30 (6)	Pt(2)–Pt(4)–Os(2)	92.42 (7)
Pt(3)–Pt(2)–Os(3)	94.70 (7)	Pt(2)–Pt(4)–Os(3)	60.32 (6)
Pt(3)–Pt(2)–Os(4)	90.42 (7)	Pt(2)–Pt(4)–Os(4)	61.51 (6)
Pt(3)–Pt(2)–Os(6)	60.87 (6)	Pt(2)–Pt(4)–Os(5)	91.33 (7)
Pt(4)–Pt(2)–Os(1)	91.79 (7)	Pt(3)–Pt(4)–Os(2)	62.31 (6)
Pt(4)–Pt(2)–Os(3)	60.19 (6)	Pt(3)–Pt(4)–Os(3)	95.01 (7)
Pt(4)–Pt(2)–Os(4)	61.74 (6)	Pt(3)–Pt(4)–Os(4)	90.48 (7)
Pt(4)–Pt(2)–Os(6)	90.49 (7)	Pt(3)–Pt(4)–Os(5)	60.81 (6)
Os(1)–Pt(2)–Os(3)	66.15 (5)	Os(2)–Pt(4)–Os(3)	66.71 (6)
Os(4)–Pt(2)–Os(6)	59.33 (5)	Os(4)–Pt(4)–Os(5)	60.33 (6)
Pt(2)–Pt(3)–Pt(4)	61.47 (6)	Os(2)–Os(1)–Os(3)	61.42 (5)
Pt(2)–Pt(3)–Os(1)	61.04 (6)	Os(1)–Os(2)–Os(3)	60.85 (5)
Pt(2)–Pt(3)–Os(2)	92.86 (6)	Os(1)–Os(3)–Os(2)	57.73 (5)
Pt(2)–Pt(3)–Os(5)	94.85 (7)	Os(5)–Os(4)–Os(6)	57.82 (6)
Pt(2)–Pt(3)–Os(6)	64.96 (6)	Os(4)–Os(5)–Os(6)	60.40 (6)
Pt(4)–Pt(3)–Os(1)	92.40 (6)	Os(4)–Os(6)–Os(5)	61.78 (6)
Pt(4)–Pt(3)–Os(2)	61.08 (6)	Os(6)–C(61)–O(61)	153 (4)
Pt(4)–Pt(3)–Os(5)	64.93 (6)	Os(5)–C(62)–O(62)	141 (4)
Pt(4)–Pt(3)–Os(6)	94.16 (7)	Os(6)–C(62)–O(62)	137 (4)
Os(1)–Pt(3)–Os(2)	62.44 (6)	M–C(av)–O	175 (5)
Os(5)–Pt(3)–Os(6)	58.84 (6)		

[a] Angles are in degrees. Estimated standard deviations in the least significant figure are given in parentheses.

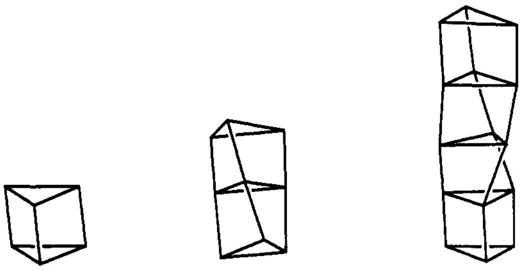

$Pt_6(CO)_6(\mu\text{-}CO)_6{}^{2-}$ $Pt_9(CO)_9(\mu\text{-}CO)_9{}^{2-}$ $Pt_{15}(CO)_{15}(\mu\text{-}CO)_{15}{}^{2-}$

Figure 2. Structures of $[Pt_3(CO)_3(\mu\text{-}CO)_3]_n{}^{2-}$ clusters.

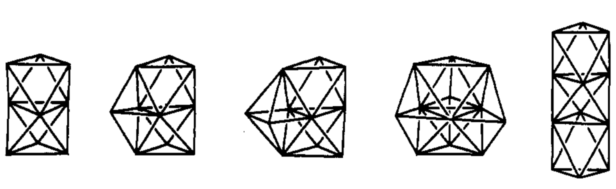

Figure 3. Structures of clusters containing stacked triangles in staggered arrangements.

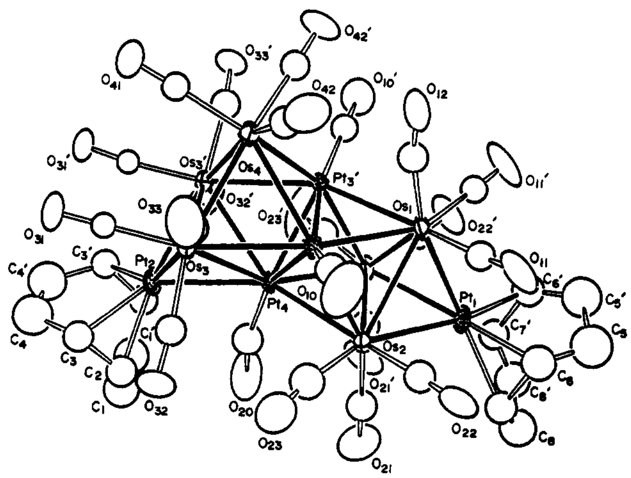

Figure 4. ORTEP diagram of $Pt_5Os_6(CO)_{21}(COD)_2$ (3), showing 50% probability thermal ellipsoids.

Table V. Positional Parameters and B(eq) Values for $Pt_5Os_6(CO)_{21}(COD)_2$ (3)

atom	x	y	z	B(eq), Å^2
Pt(1)	0.95223 (11)	$^1/_4$	1.04807 (09)	4.23 (6)
Pt(2)	0.59865 (11)	$^1/_4$	0.51875 (09)	3.76 (6)
Pt(3)	0.59565 (07)	0.16770 (05)	0.84526 (06)	2.92 (4)
Pt(4)	0.70091 (09)	$^1/_4$	0.72653 (08)	2.69 (5)
Os(1)	0.71244 (11)	$^1/_4$	1.01433 (09)	3.45 (6)
Os(2)	0.83098 (07)	0.15871 (06)	0.88380 (06)	3.55 (4)
Os(3)	0.49030 (07)	0.16267 (05)	0.64094 (06)	2.96 (4)
Os(4)	0.38321 (10)	$^1/_4$	0.77283 (09)	3.73 (6)

O)$_{21}$(COD)$_2$ (3), and $Pt_4Os_6(CO)_{19}(COD)_2$ (4) in the yields of 17%, 13%, and 9%, respectively. Several minor products $PtOs_2(CO)_8(COD)$,[6a] $Pt_2Os_4(CO)_{18}$,[10] $Pt_2Os_4(CO)_{17}$,[6d] $Pt_2Os_4(CO)_{12}(COD)_2$,[6a] and $Pt_2Os_6(CO)_{17}(COD)_2$[5a] were also obtained. The CO atmosphere was found to give higher yields of compounds **2** and **3**. Compounds **2**–**4** were characterized by a combination of IR, ^{1}H NMR, and single-crystal X-ray diffraction analyses.

An ORTEP diagram of the structure of **2** is shown in Figure 1. Final atom positional parameters are listed in Table II. Selected interatomic distances and angles are listed in Tables III and IV. It is not possible to distinguish platinum from osmium by X-ray crystallographic methods. The presence of four platinum atoms in the complex was determined by elemental analysis. The assignment of the platinum sites in the structure was determined by geometric and coordination considerations. For example, since platinum contains two more electrons than osmium, platinum atoms in complexes should have fewer ligands; see below. The cluster of **2** can be described as two Pt_3Os_3 octahedra sharing the triplatinum triangular face. One of the Os_3 triangular faces, Os(1)–Os(2)–Os(3), is capped by a Pt(COD) grouping. The atoms of the Pt_3 triangle each have only one carbonyl ligand, while each osmium atom contains three terminal CO ligands. There is also one CO ligand, C(62)–O(62), bridging the Os(4)–Os(5) bond. The three triangles Os(1)–Os(2)–Os(3), Pt(2)–Pt(3)–Pt(4), and Os(4)–Os(5)–Os(6) have a staggered face-to-face stacking. The average Pt–Pt distance in **2**, 2.65 Å, is significantly shorter than the average Os–Os distance, 2.90 Å, but is similar to the Pt–Pt distances observed in the platinum anions $[Pt_3(CO)_3(\mu\text{-}CO)_3]_n{}^{2-}$ (n = 2–5) that were studied by Chini and Dahl.[12] The Os_3–Pt_3 interlayer spacing to the platinum-capped Os_3 triangle, 2.22 Å, is slightly smaller than that to the uncapped Os_3 triangle, 2.39 Å. The reason for this is not clear, but it may be related to the longer Os–Os distances, 2.96 Å, in the capped Os_3 triangle compared with those of uncapped Os_3 triangle, 2.85 Å. The average Os–Os distance in $Os_3(CO)_{12}$ is 2.877 Å. The molecule contains a total of 136 valence electrons, which is exactly the value expected for the two face-shared octahedra with one capping group.[13]

The staggered stacking in **2** contrasts with the nearly eclipsed stacking of the Pt_3 triangles in the anions $[Pt_3(CO)_3(\mu\text{-}CO)_3]_n{}^{2-}$ (n = 2–5) (Figure 2).[12] Staggered face-to-face stacking was observed in the anionic complexes $[Rh_9(CO)_{19}]^{3-}$[14] and $[PtRh_8(CO)_{19}]^{2-}$[3c] (A). In $[PtRh_8(CO)_{18}]^{2-}$[3c] the platinum atom lies in one of the sites of the central triangle. The structures of these and some other high-nuclearity cluster complexes exhibiting stacked triangular layers with staggered arrangements of the metal atoms are shown in Figure 3. $[Rh_{10}(CO)_{21}]^{2-}$[15] contains two face-fused octahedra with a μ_4-bridging group (B). $[Rh_{11}(CO)_{23}]^{3-}$[16] and $[Pt_2Rh_9(CO)_{22}]^{3-}$[3a] are isostructural and consist

---

(12) (a) Longoni, G.; Chini, P. *J. Am. Chem. Soc.* **1976**, *98*, 7225. (b) Calabrese, J. C.; Dahl, L. F.; Chini, P.; Longoni, G.; Martinengo, S. *J. Am. Chem. Soc.* **1974**, *96*, 2614.

(13) Mingos, D. M. P.; May, A. S. In *The Chemistry of Metal Cluster Complexes*; Shriver, D. F., Kaesz, H. D., Adams, R. D., Eds.; VCH Publishers: New york, 1990; Chapter 2.

(14) Martinengo, S.; Fumagalli, A.; Bonfichi, R.; Ciani, G.; Sironi, A. *J. Chem. Soc., Chem. Commun.* **1982**, 825.

(15) Martinengo, S.; Ciani, G.; Sironi, A. *J. Chem. Soc., Chem. Commun.* **1986**, 1282.

(16) Martinengo, S.; Fumagalli, A.; Ciani, G.; Sironi, A. *J. Chem. Soc., Chem. Commun.* **1983**, 453.

Table VI. Intramolecular Distances for 3[a]

Pt(1)–Os(1)	2.808 (3)	Os(1)–Os(2)	2.949 (2)
Pt(1)–Os(2)	2.809 (2)	Os(1)–C(11)	1.87 (3)
Pt(1)–C(6)	2.21 (5)	Os(1)–C(12)	1.85 (4)
Pt(1)–C(7)	2.27 (4)	Os(2)–Os(2)′	2.923 (3)
Pt(2)–Pt(4)	2.857 (2)	Os(2)–C(21)	1.88 (3)
Pt(2)–Os(3)	2.755 (2)	Os(2)–C(22)	1.86 (3)
Pt(2)–C(2)	2.24 (3)	Os(2)–C(23)	1.88 (3)
Pt(2)–C(3)	2.21 (3)	Os(3)–Os(3)′	2.796 (2)
Pt(3)–Pt(3)′	2.635 (2)	Os(3)–Os(4)	2.846 (2)
Pt(3)–Pt(4)	2.657 (2)	Os(3)–C(31)	1.88 (2)
Pt(3)–Os(1)	2.767 (2)	Os(3)–C(32)	1.89 (3)
Pt(3)–Os(2)	2.755 (2)	Os(3)–C(33)	1.96 (3)
Pt(3)–Os(3)	2.822 (2)	Os(4)–C(41)	1.91 (4)
Pt(3)–Os(4)	2.837 (2)	Os(4)–C(42)	1.92 (3)
Pt(3)–C(10)	1.86 (3)	C(2)–C(3)	1.40 (3)
Pt(4)–Os(2)	2.781 (2)	C(6)–C(7)	1.60 (6)
Pt(4)–Os(3)	2.889 (2)	O–C(av)	1.15 (4)
Pt(4)–C(20)	1.87 (5)		

[a] Distances are in angstroms. Estimated standard deviations in the least significant figure are given in parentheses.

Table VII. Intramolecular Bond Angles for 3[a]

Pt(3)–Pt(3)′–Pt(4)	60.27 (3)	Pt(2)–Pt(4)–Os(2)	145.17 (4)
Pt(3)–Pt(3)′–Os(1)	61.57 (3)	Pt(2)–Pt(4)–Os(3)	57.31 (5)
Pt(3)–Pt(3)′–Os(2)	93.00 (3)	Pt(3)–Pt(4)–Pt(3)′	59.47 (6)
Pt(3)–Pt(3)′–Os(3)	91.63 (3)	Pt(3)–Pt(4)–Os(2)	91.95 (6)
Pt(3)–Pt(3)′–Os(4)	62.32 (3)	Pt(3)–Pt(4)–Os(3)	89.73 (6)
Pt(4)–Pt(3)–Os(1)	94.08 (6)	Pt(3)–Pt(4)–Os(2)	91.95 (6)
Pt(4)–Pt(3)–Os(2)	61.81 (5)	Pt(3)–Pt(4)–Os(3)	61.01 (5)
Pt(4)–Pt(3)–Os(3)	63.56 (5)	Os(2)–Pt(4)–Os(2)	63.42 (6)
Pt(4)–Pt(3)–Os(4)	94.07 (6)	Os(2)–Pt(4)–Os(3)	148.39 (5)
Os(1)–Pt(3)–Os(2)	64.54 (5)	Os(2)–Pt(4)–Os(3)	148.39 (5)
Os(1)–Pt(3)–Os(3)	152.08 (4)	Os(2)–Os(1)–Os(2)′	59.43 (6)
Os(1)–Pt(3)–Os(4)	108.17 (6)	Os(1)–Os(2)–Os(2)′	60.28 (3)
Os(2)–Pt(3)–Os(3)	112.83 (6)	Os(3)–Os(3)′–Os(4)	60.58 (3)
Os(2)–Pt(3)–Os(4)	152.79 (5)	Os(3)–Os(4)–Os(3)	58.84 (6)
Os(3)–Pt(3)–Os(4)	60.39 (5)	Pt(4)–C(20)–O(20)	165 (4)
Pt(2)–Pt(4)–Pt(3)	118.31 (6)	M–C(av)–O	175 (4)

[a] Angles are in degrees. Estimated standard deviations in the least significant figure are given in parentheses.

of three face-shared octahedra (C). In $[Pt_2Rh_9(CO)_{22}]^{3-}$ the platinum atoms occupy the sites of highest connectivity. $[Ni_{12}(CO)_{21}(H)_{4-n}]^{n-}$[17] and $[Pt_3Ni_9(CO)_{21}(H)_{4-n}]^{n-}$[4c] ($n = 2$–4) have similar structures with three μ_4-bridging groups (D). In the platinum–nickel cluster the platinum atoms form the central triangle. In these complexes the hydride ligands are located in interstitial octahedral holes. Only two complexes $[Ir_{12}(CO)_{26}]^{2-}$[18a] and $H_2Rh_{12}(CO)_{25}$[18b] have structures with four stacked triangular layers in the staggered arrangement (E).

An ORTEP diagram of the structure of **3** is shown in Figure 4. Final atom positional parameters are listed in Table V. Selected interatomic distances and angles are listed in Tables VI and VII. The structure of compound **3** is very similar to that of **2**, except that the bridging CO in compound **2** is replaced by a Pt(COD) group that caps one face of Pt(4)–Os(3)–Os(3′) triangle between the Pt_3 and uncapped Os_3 triangles. The molecule contains a crystallographically imposed symmetry plane that passes through the metal atoms Pt(1), Os(1), Pt(4), Os(4), and Pt(2). The Os_3–Pt_3 interlayer spacings in **3**, 2.24 and 2.36 Å, are very similar to those in **2** indicating that the addition of the Pt(COD) capping group on the Pt(4), Os(3), Os(3′) triangle does not produce a significant effect on the associated interlayer spacing. The cluster contains a total of 148 valence electrons, which is exactly the value expected for the doubly capped cluster of two face-shared octahedra.[13]

It is easy to imagine the formation of **3** from **2** by substitution of the bridging CO ligand with a Pt(COD) grouping. This was accomplished albeit in a low yield (6%) in an independent experiment by activating **2** with Me_3NO in the presence of $Pt(COD)_2$. Interestingly, a new high-nuclearity platinum–osmium carbonyl cluster complex $Pt_7Os_6(CO)_{21}(COD)_2$ (**5**) was also obtained from this reaction in an 8% yield. Compound **5** was characterized by a combination of IR, ^1H NMR, and single-crystal X-ray diffraction analyses and will be described below.

An ORTEP diagram of the structure of **4** is shown in Figure 5. Final atom positional parameters are listed in Table VIII. Se-

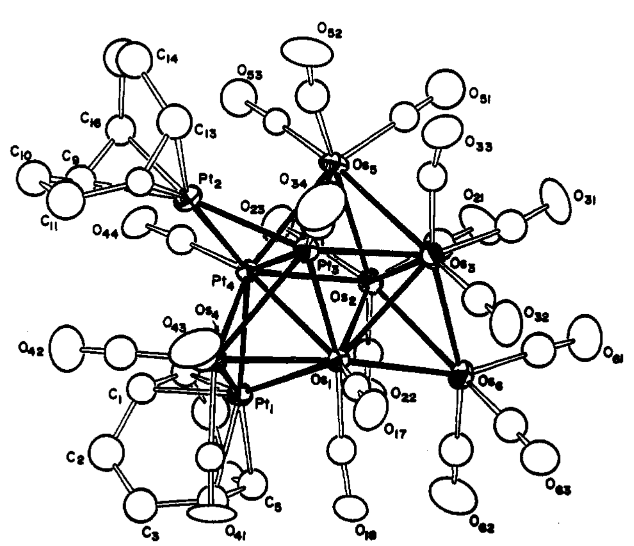

Figure 5. ORTEP diagram of $Pt_4Os_6(CO)_{19}(COD)_2$ (**4**), showing 50% probability thermal ellipsoids.

Table VIII. Positional Parameters and *B*(eq) Values for $Pt_4Os_6(CO)_{19}(C_8H_{12})_2$ (**4**)

atom	*x*	*y*	*z*	*B*(eq), Å^2
Pt(1)	0.073 09 (03)	0.128 26 (09)	0.079 89 (05)	2.34 (5)
Pt(2)	0.181 78 (03)	0.119 25 (09)	0.123 58 (05)	2.43 (5)
Pt(3)	0.158 81 (03)	0.210 67 (08)	−0.006 57 (05)	2.20 (5)
Pt(4)	0.127 41 (02)	0.209 40 (08)	0.109 31 (05)	1.87 (4)
Os(1)	0.098 84 (03)	0.219 20 (08)	−0.037 28 (05)	2.08 (5)
Os(2)	0.096 58 (03)	0.411 83 (09)	0.055 99 (05)	2.49 (5)
Os(3)	0.132 20 (03)	0.411 06 (09)	−0.064 44 (05)	2.64 (5)
Os(4)	0.123 84 (03)	0.019 95 (08)	0.015 70 (05)	2.30 (5)
Os(5)	0.160 32 (03)	0.404 49 (09)	0.097 37 (05)	2.62 (5)
Os(6)	0.069 70 (03)	0.406 18 (09)	−0.104 12 (06)	3.16 (6)

Table IX. Intramolecular Distances for **4**[a]

Pt(1)–Pt(4)	2.634 (2)	Os(2)–Os(5)	2.889 (2)
Pt(1)–Os(1)	2.734 (1)	Os(2)–Os(6)	2.870 (2)
Pt(1)–Os(4)	3.014 (2)	Os(2)–C(21)	1.87 (3)
Pt(2)–Pt(3)	2.584 (1)	Os(2)–C(22)	1.87 (3)
Pt(2)–Pt(4)	2.678 (2)	Os(2)–C(23)	1.89 (2)
Pt(2)–Os(4)	3.219 (2)	Os(3)–Os(5)	2.913 (2)
Pt(2)–Os(5)	3.525 (2)	Os(3)–Os(6)	2.830 (2)
Pt(3)–Pt(4)	2.656 (1)	Os(3)–C(31)	1.89 (3)
Pt(3)–Os(1)	2.709 (2)	Os(3)–C(32)	1.89 (3)
Pt(3)–Os(3)	2.781 (2)	Os(3)–C(33)	1.95 (3)
Pt(3)–Os(4)	2.827 (2)	Os(4)–C(41)	1.91 (3)
Pt(3)–Os(5)	2.918 (2)	Os(4)–C(42)	1.89 (3)
Pt(3)–C(34)	1.85 (3)	Os(4)–C(43)	1.86 (3)
Pt(4)–Os(1)	2.684 (1)	Os(5)–C(51)	1.86 (3)
Pt(4)–Os(2)	2.860 (2)	Os(5)–C(52)	1.95 (4)
Pt(4)–Os(4)	2.764 (1)	Os(5)–C(53)	1.84 (2)
Pt(4)–Os(5)	2.781 (2)	Os(6)–C(61)	1.90 (3)
Pt(4)–C(44)	1.84 (2)	Os(6)–C(62)	1.89 (4)
Os(1)–Os(2)	2.812 (2)	Os(6)–C(63)	1.85 (3)
Os(1)–Os(3)	2.816 (2)	C(1)–C(8)	1.32 (3)
Os(1)–Os(4)	2.718 (2)	C(4)–C(5)	1.39 (4)
Os(1)–Os(6)	2.746 (2)	C(9)–C(16)	1.36 (4)
Os(1)–C(17)	1.92 (2)	C(12)–C(13)	1.37 (3)
Os(1)–C(18)	1.86 (3)	O–C(av)	1.15 (4)
Os(2)–Os(3)	2.852 (2)		

[a] Distances are in angstroms. Estimated standard deviations in the least significant figure are given in parentheses.

---

(17) Broach, R. W.; Dahl, L. F.; Longoni, G.; Chini, P.; Schultz, A. J.; Williams, J. M. *Adv. Chem. Ser.* **1978**, *No. 167*, 93.

(18) Pergola, R. D.; Demartin, F.; Garlaschelli, L.; Manassero, M.; Martinengo, S.; Sansoni, M. *Inorg. Chem.* **1987**, *26*, 3487. (b) Martinengo, S.; Ciani, G.; Sironi, A. *J. Chem. Soc., Chem. Commun.* **1985**, 1757.

Table X. Intramolecular Bond Angles[a]

Pt(3)–Pt(2)–Pt(4)	60.60 (4)	Pt(1)–Pt(4)–Os(5)	142.34 (5)
Pt(2)–Pt(3)–Pt(4)	61.45 (4)	Pt(2)–Pt(4)–Pt(3)	57.95 (4)
Pt(2)–Pt(3)–Os(1)	116.59 (5)	Pt(2)–Pt(4)–Os(1)	114.23 (5)
Pt(2)–Pt(3)–Os(3)	140.34 (5)	Pt(2)–Pt(4)–Os(2)	140.00 (5)
Pt(2)–Pt(3)–Os(4)	72.84 (4)	Pt(2)–Pt(4)–Os(4)	72.50 (4)
Pt(2)–Pt(3)–Os(5)	79.43 (4)	Pt(2)–Pt(4)–Os(5)	80.42 (5)
Pt(4)–Pt(3)–Os(1)	60.04 (4)	Pt(3)–Pt(4)–Os(1)	60.95 (4)
Pt(4)–Pt(3)–Os(3)	91.36 (5)	Pt(3)–Pt(4)–Os(2)	92.57 (4)
Pt(4)–Pt(3)–Os(4)	60.44 (4)	Pt(3)–Pt(4)–Os(4)	62.85 (4)
Pt(4)–Pt(3)–Os(5)	59.63 (4)	Pt(3)–Pt(4)–Os(5)	64.88 (4)
Os(1)–Pt(3)–Os(3)	61.70 (4)	Os(1)–Pt(4)–Os(2)	60.87 (4)
Os(1)–Pt(3)–Os(4)	58.77 (4)	Os(1)–Pt(4)–Os(4)	59.83 (4)
Os(1)–Pt(3)–Os(5)	91.03 (5)	Os(1)–Pt(4)–Os(5)	94.61 (4)
Os(3)–Pt(3)–Os(4)	120.45 (6)	Os(2)–Pt(4)–Os(4)	120.49 (5)
Os(3)–Pt(3)–Os(5)	61.41 (4)	Os(2)–Pt(4)–Os(5)	61.59 (4)
Os(4)–Pt(3)–Os(5)	120.07 (5)	Os(4)–Pt(4)–Os(5)	127.72 (5)
Pt(1)–Pt(4)–Pt(2)	134.74 (5)	Os(2)–Os(1)–Os(3)	60.89 (4)
Pt(1)–Pt(4)–Pt(3)	117.28 (5)	Os(1)–Os(2)–Os(3)	59.62 (4)
Pt(1)–Pt(4)–Os(1)	61.85 (4)	Os(1)–Os(3)–Os(2)	59.49 (4)
Pt(1)–Pt(4)–Os(2)	80.89 (5)	M–C(av)–O	174 (3)
Pt(1)–Pt(4)–Os(4)	67.84 (4)		

[a] Angles are in degrees. Estimated standard deviations in the least significant figure are given in parentheses.

Table XI. Positional Parameters and *B*(eq) Values for $Pt_7Os_6(CO)_{21}(C_8H_{12})_2$ (**5**)

atom	*x*	*y*	*z*	*B*(eq), Å²
Pt(1)	0.595 66 (07)	0.344 56 (12)	0.679 98 (07)	2.36 (7)
Pt(2)	0.738 43 (08)	0.057 91 (12)	0.412 07 (07)	2.68 (8)
Pt(3)	0.811 03 (08)	0.323 74 (14)	0.495 96 (08)	3.53 (8)
Pt(4)	0.728 83 (08)	0.045 47 (12)	0.541 08 (07)	2.95 (8)
Pt(5)	0.665 79 (07)	0.226 66 (12)	0.484 25 (07)	2.19 (7)
Pt(6)	0.720 50 (07)	0.429 52 (11)	0.509 39 (07)	2.26 (7)
Pt(7)	0.775 57 (07)	0.252 51 (12)	0.561 41 (07)	2.24 (7)
Os(1)	0.820 18 (08)	0.482 98 (13)	0.431 73 (08)	3.22 (8)
Os(2)	0.664 62 (07)	0.182 11 (12)	0.608 20 (07)	2.20 (7)
Os(3)	0.845 10 (08)	0.104 85 (13)	0.488 61 (08)	3.11 (8)
Os(4)	0.599 98 (07)	0.376 55 (12)	0.553 34 (07)	2.34 (7)
Os(5)	0.774 73 (07)	0.273 67 (12)	0.431 88 (07)	2.24 (7)
Os(6)	0.714 43 (07)	0.399 59 (12)	0.638 98 (07)	2.22 (7)

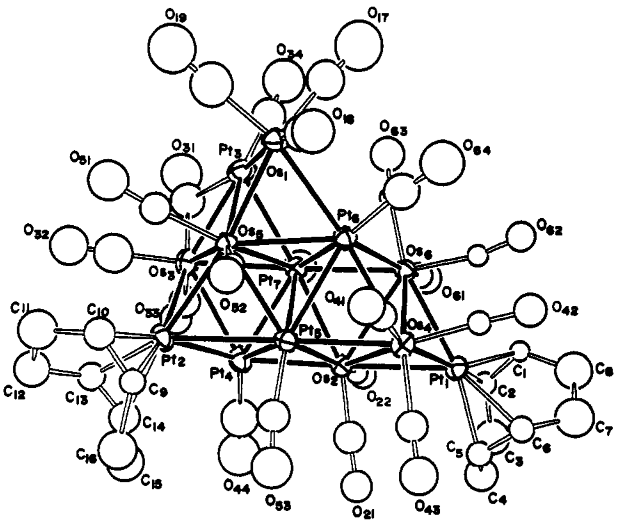

Figure 6. ORTEP diagram of $Pt_7Os_6(CO)_{21}(COD)_2$ (**5**), showing 50% probability thermal ellipsoids.

Table XII. Intramolecular Distances for **5**[a]

Pt(1)–Os(2)	2.911 (2)	Pt(5)–Os(4)	2.743 (2)
Pt(1)–Os(4)	2.736 (2)	Pt(5)–Os(5)	2.650 (3)
Pt(1)–Os(5)	2.761 (2)	Pt(6)–Pt(7)	2.658 (2)
Pt(2)–Pt(4)	2.773 (3)	Pt(6)–Os(1)	2.797 (3)
Pt(2)–Pt(5)	3.008 (2)	Pt(6)–Os(4)	2.812 (3)
Pt(2)–Os(3)	2.788 (2)	Pt(6)–Os(5)	2.780 (2)
Pt(2)–Os(5)	2.746 (2)	Pt(6)–Os(6)	2.798 (2)
Pt(3)–Pt(7)	2.802 (3)	Pt(7)–Os(2)	2.711 (2)
Pt(3)–Os(1)	2.665 (2)	Pt(7)–Os(3)	2.812 (3)
Pt(3)–Os(3)	2.755 (3)	Pt(7)–Os(5)	2.777 (2)
Pt(3)–Os(5)	2.651 (2)	Pt(7)–Os(6)	2.777 (2)
Pt(4)–Pt(5)	2.813 (2)	Os(1)–Os(5)	2.705 (2)
Pt(4)–Pt(7)	2.718 (2)	Os(2)–Os(4)	2.938 (2)
Pt(4)–Os(2)	2.598 (2)	Os(2)–Os(6)	2.897 (2)
Pt(4)–Os(3)	2.822 (3)	Os(3)–Os(5)	2.774 (2)
Pt(5)–Pt(6)	2.754 (2)	Os(4)–Os(6)	2.986 (2)
Pt(5)–Pt(7)	2.808 (2)	O–C(av)	1.180 (7)
Pt(5)–Os(2)	2.701 (2)		

[a] Distances are in angstroms. Estimated standard deviations in the least significant figure are given in parentheses.

Table XIII. Intramolecular Bond Angles for **5**[a]

Pt(4)–Pt(2)–Pt(5)	58.07 (6)	Pt(7)–Pt(5)–Os(5)	61.08 (6)
Pt(4)–Pt(2)–Os(3)	60.99 (6)	Os(2)–Pt(5)–Os(4)	65.32 (6)
Pt(4)–Pt(2)–Os(5)	85.89 (6)	Pt(5)–Pt(6)–Pt(7)	62.48 (5)
Pt(5)–Pt(2)–Os(3)	88.61 (6)	Pt(5)–Pt(6)–Os(4)	59.06 (6)
Pt(5)–Pt(2)–Os(5)	54.62 (6)	Pt(5)–Pt(6)–Os(5)	57.22 (6)
Os(3)–Pt(2)–Os(5)	60.17 (5)	Pt(7)–Pt(6)–Os(4)	93.61 (7)
Os(1)–Pt(3)–Os(3)	122.57 (7)	Pt(7)–Pt(6)–Os(5)	61.36 (6)
Os(1)–Pt(3)–Os(5)	61.17 (6)	Pt(7)–Pt(6)–Os(6)	61.15 (6)
Os(3)–Pt(3)–Os(5)	61.72 (5)	Os(1)–Pt(6)–Os(5)	58.03 (6)
Pt(5)–Pt(4)–Pt(7)	60.98 (5)	Os(4)–Pt(6)–Os(6)	64.32 (6)
Pt(2)–Pt(5)–Pt(4)	56.78 (6)	Pt(3)–Pt(7)–Os(3)	58.77 (6)
Pt(2)–Pt(5)–Pt(7)	87.29 (6)	Pt(3)–Pt(7)–Os(5)	56.75 (6)
Pt(2)–Pt(5)–Os(5)	57.66 (6)	Pt(4)–Pt(7)–Pt(5)	61.18 (5)
Pt(4)–Pt(5)–Pt(7)	57.84 (5)	Pt(3)–Os(1)–Os(5)	59.17 (6)
Pt(4)–Pt(5)–Os(2)	56.17 (6)	Os(4)–Os(2)–Os(6)	61.54 (5)
Pt(6)–Pt(5)–Pt(7)	57.09 (5)	Os(2)–Os(4)–Os(6)	58.55 (5)
Pt(6)–Pt(5)–Os(4)	61.52 (6)	Os(2)–Os(6)–Os(4)	59.91 (5)
Pt(6)–Pt(5)–Os(5)	61.89 (6)	M–C(av)–O	175 (5)
Pt(7)–Pt(5)–Os(2)	58.93 (6)		

[a] Angles are in degrees. Estimated standard deviations in the least significant figure are given in parentheses.

lected interatomic distances and angles are listed in Tables IX and X. Compound **4** can be viewed as a meta-bicapped Pt_2Os_4 octahedron. The Os(1), Os(2), Os(3) triangle is capped by an $Os(CO)_3$ group, and the Os(1), Pt(3), Pt(4) triangle is capped by an $Os(CO)_2$ group which contains a capping group Pt(COD) on the Os(1), Os(4), Pt(4) triangle. The most unusual grouping is a Pt(COD) group that bridges only two metal atoms, Pt(3) and Pt(4), Pt(2)–Pt(3) = 2.584(1) Å and Pt(2)–Pt(4) = 2.678 (2) Å. The distances Pt(2)···Os(4) and Pt(2)···Os(5), 3.219 and 3.525 Å, respectively, are too long to contain significant bonding interactions. The Pt(2)–Pt(3)–Pt(4) triangle is nearly perpendicular, 94.40°, to the Pt_2Os_2 plane. Although 16-electron Pt(COD) groupings are known to bridge di- and trinuclear metal assemblies, this is the first example of such an arrangement on a tetranuclear metal site. The planarity of this Pt_2Os_2 tetranuclear site suggests that it might be a reasonable model for bonding of Pt(COD) groupings to metal surfaces and also suggests that this arrangement might exist on metal surfaces when the surface contains a substantial ligand coverage. As in **2** and **3**, the two platinum atoms that do not contain COD ligands each contain only one linear terminal carbonyl ligand. Each osmium has three carbonyl ligands, except for Os(1), which is located at a site of high connectivity and has only two CO ligands. The average Pt–Pt distance, 2.64 Å, is much shorter than the average Os–Os distance, 2.83 Å, but is similar to the Pt–Pt distances found in compounds **2** and **3**. The cluster has a total of 134 valence electrons, which is two less than the value expected for face-fused octahedral and trigonal bipyramidal clusters containing one capping and one bridging group.[13] The electron deficiency is probably associated with the edge-bridging Pt(COD) grouping that has only a 16-electron configuration. Similar electron deficiencies in related cluster complexes containing platinum have been rationalized by Mingos.[19]

Compounds **2** and **4** both contain the same numbers of platinum and osmium atoms, but **2** has three more carbonyl ligands and one less COD than **4**. Accordingly, we attempted to convert of

---

(19) Mingos, D. M. P.; Evans, D. G. *J. Organomet. Chem.* **1983**, *251*, C13.

Scheme I

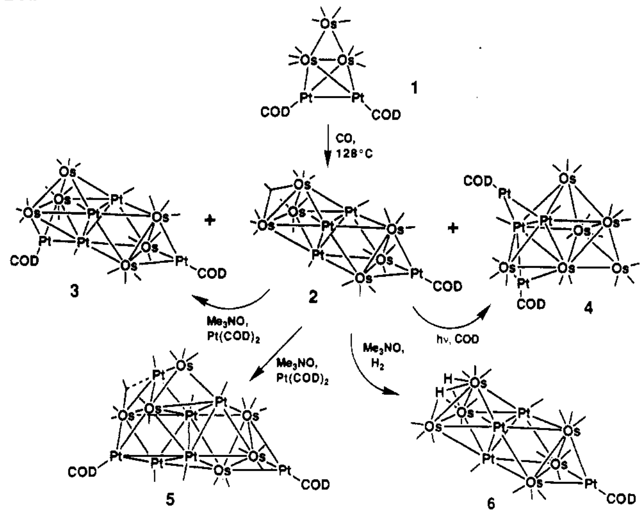

2 to **4** by a photodecarbonylation process in the presence of COD. This reaction was found to proceed in a fairly good yield (65%). In the transformation of **2** to **4** the COD ligand was added to one of the platinum atoms of the Pt_3 triangle. Presumably, the resultant steric crowding made the layerlike structure of **2** unfavorable, and the Pt_3 triangle was pulled out from between the two Os_3 layers. In the absence of isolable intermediates it is difficult to predict other details of the transformation.

On the basis of elemental analysis for platinum, compound **5** was determined to contain seven platinum atoms. An ORTEP diagram of the structure of **5** is shown in Figure 6. Final atom positional parameters are listed in Table XI. Selected interatomic distances and angles are listed in Tables XII and XIII. The four metal atoms containing only one carbonyl ligand, Pt(4), Pt(5), Pt(6), and Pt(7), were assigned as platinum in analogy with compounds **2** and **3**. The two metal atoms containing the COD ligands, Pt(1) and Pt(2), were also assigned as platinum, and finally the metal atom Pt(3) was assigned as platinum since this atom lies in a site of low metal connectivity and contains only one terminal CO ligand although one of the CO ligands on atom Os(3), C(31)–O(31), does form a strong semibridging coordination to it. All osmium atoms have three carbonyl ligands except atoms Os(2) and Os(5), which lie on sites of very high metal connectivity and have only two carbonyl ligands. The layerlike structure of the metal atoms in readily apparent in Figure 6. The platinum-capped Os_3 triangle sits next to a planar Pt_4 layer, which in turn lies next to a planar five atom Os_3Pt_2 layer on the far left in Figure 6. The latter contains a rare example of a Pt(COD) grouping bonded to four other metal atoms. The average Os–Os distance, 2.86 Å, is similar to that in **2** and **3**, but the average Pt–Pt distance, 2.79 Å, is about 0.15 Å longer. The Pt(2)–Pt(5) distance, 3.008 (2) Å, the longest bonding distance in this cluster, involves the unusual μ_4-Pt(COD) bridging group, Pt(2).

We recently reported the formation of the compound $Pt_4Os_6(CO)_{21}(COD)(\mu\text{-}H)_2$ (**6**) from the pyrolysis of $Pt_2Os_3(CO)_9(COD)_2(\mu\text{-}H)_2$.[6c] Compound **6** is structurally very similar to compound **2**, except that it has two bridging hydride ligands in place of the bridging CO group. We have found that **2** can be converted to **6** in 79% yield by decarbonylation with Me_3NO in the presence of hydrogen.

Summary

The results of this study are summarized in Scheme I. The pyrolysis of compound **1** yielded three high-nuclearity cluster compounds **2**–**4**. Compound **2** assumed a central role in this study. When photolyzed in the presence of COD, it yielded compound **4**. It also yielded the higher nuclearity clusters **3** and **5**, by reaction with $Pt(COD)_2$ when decarbonylated by Me_3NO. It yielded **6** if the Me_3NO decarbonylation was performed under an atmosphere of hydrogen.

A notable feature of the structures of compounds **2**, **3**, and **6** is the segregation of the platinum and osmium into alternating layers of the pure elements. It may be possible to extend the stacking of these clusters. It will be of interest to see if the preference for segregated stacking is maintained.

Acknowledgment. These studies were supported by the National Science Foundation under Grant No. CHE-8919786.

Supplementary Material Available: Complete listings of positional parameters and tables of bond distances and angles and anisotropic thermal parameters (37 pages); tables of structure factor amplitudes (45 pages). Ordering information is given on any current masthead page. Hydrogen atom parameters, anisotropic thermal parameters, and structure factor amplitudes for **2** and **3** were deposited previously.[6b]